Am J Physiol Lung Cell Mol Physiol 315: L348–L359, 2018.
First published May 3, 2018; doi:10.1152/ajplung.00052.2018.

RESEARCH ARTICLE

Intrauterine growth restriction decreases NF-κB signaling in fetal pulmonary artery endothelial cells of fetal sheep

R. Blair Dodson,[1,2,3,4,6] Kyle N. Powers,[1,2,3] Jason Gien,[2,4] Paul J. Rozance,[4] Gregory Seedorf,[2,5] David Astling,[6] Kenneth Jones,[6] Timothy M. Crombleholme,[1,3] Steven H. Abman,[2,4] and Cristina M. Alvira[7]

[1]*Laboratory for Fetal and Regenerative Biology, University of Colorado Denver Anschutz Medical Campus, Aurora, Colorado;* [2]*Pediatric Heart Lung Center, University of Colorado Denver Anschutz Medical Campus, Aurora, Colorado;* [3]*Department of Surgery, University of Colorado Denver Anschutz Medical Campus, Aurora, Colorado;* [4]*Department of Pediatrics, University of Colorado Denver Anschutz Medical Campus, Aurora, Colorado;* [5]*Department of Biochemistry and Molecular Genetics, University of Colorado Denver Anschutz Medical Campus, Aurora, Colorado;* [6]*United Therapeutics, Regenerative Medicine Laboratory, Research Triangle Park, Durham, North Carolina; and* [7]*Department of Pediatrics, Stanford University School of Medicine, Palo Alto, California*

Submitted 31 January 2018; accepted in final form 2 May 2018

Dodson RB, Powers KN, Gien J, Rozance PJ, Seedorf G, Astling D, Jones K, Crombleholme TM, Abman SH, Alvira CM. Intrauterine growth restriction decreases NF-κB signaling in fetal pulmonary artery endothelial cells of fetal sheep. *Am J Physiol Lung Cell Mol Physiol* 315: L348–L359, 2018. First published May 3, 2018; doi:10.1152/ajplung.00052.2018.—Intrauterine growth restriction (IUGR) in premature newborns increases the risk for bronchopulmonary dysplasia, a chronic lung disease characterized by disrupted pulmonary angiogenesis and alveolarization. We previously showed that experimental IUGR impairs angiogenesis; however, mechanisms that impair pulmonary artery endothelial cell (PAEC) function are uncertain. The NF-κB pathway promotes vascular growth in the developing mouse lung, and we hypothesized that IUGR disrupts NF-κB-regulated proangiogenic targets in fetal PAEC. PAECs were isolated from the lungs of control fetal sheep and sheep with experimental IUGR from an established model of chronic placental insufficiency. Microarray analysis identified suppression of NF-κB signaling and significant alterations in extracellular matrix (ECM) pathways in IUGR PAEC, including decreases in collagen 4α1 and laminin α4, components of the basement membrane and putative NF-κB targets. In comparison with controls, immunostaining of active NF-κB complexes, NF-κB-DNA binding, baseline expression of NF-κB subunits p65 and p50, and LPS-mediated inducible activation of NF-κB signaling were decreased in IUGR PAEC. Although pharmacological NF-κB inhibition did not affect angiogenic function in IUGR PAEC, angiogenic function of control PAEC was reduced to a similar degree as that observed in IUGR PAEC. These data identify reductions in endothelial NF-κB signaling as central to the disrupted angiogenesis observed in IUGR, likely by impairing both intrinsic PAEC angiogenic function and NF-κB-mediated regulation of ECM components necessary for vascular development. These data further suggest that strategies that preserve endothelial NF-κB activation may be useful in lung diseases marked by disrupted angiogenesis such as IUGR.

alveolarization; angiogenesis; bronchopulmonary dysplasia; extracellular matrix

INTRODUCTION

Intrauterine growth restriction (IUGR) is a multifactorial disease resulting from maternal, placental, or fetal factors, which culminate in decreased nutrient and oxygen supply and hemodynamic stress to the developing fetus (20). IUGR is the second leading cause of prematurity and increases the risk of additional adverse perinatal and neonatal outcomes, including stillbirth, necrotizing enterocolitis (48, 65), retinopathy of prematurity (18, 37, 42, 48), and bronchopulmonary dysplasia (BPD) (11, 62, 67). The growth-restricted fetus is exposed to significant metabolic, hormonal, and hemodynamic alterations of the intrauterine environment that have detrimental effects on fetal organ development and increase the risk for adult disorders, including diabetes mellitus, hypertension, and coronary artery disease (20, 66).

Previous studies have shown that physiological changes in the fetal lung that are associated with IUGR are likely related to disruption of several developmental pathways, including surfactant synthesis (15, 36, 44) and decreased epithelial cell differentiation (17). In addition, rats with experimental IUGR have decreased alveolar and vascular growth, which may be due to downregulation of vascular endothelial growth factor (VEGF), a potent proangiogenic factor (47) and elastin deposition (33). In a fetal sheep model of IUGR induced by utero-placental embolization, lung diffusion capacity and compliance are significantly decreased in 8-wk-old sheep (34), and fewer and larger alveoli are observed in IUGR sheep at 2 yr of age (51). Similarly, clinical studies have shown that IUGR adversely affects both short- and long-term respiratory outcomes. In premature infants, growth restriction is an independent risk factor for the development of BPD (11, 60, 62) and may represent an even stronger risk factor than extreme prematurity for BPD and respiratory disease during early childhood (67). Lower birth weight has also been associated with an increased risk of asthma in children and chronic obstructive pulmonary disease in adults, suggesting an incomplete capacity of lung growth to compensate for antenatal disruptions in lung development because of IUGR (5, 21, 49, 53).

Address for reprint requests and other correspondence: R. B. Dodson, 2 Maughan Dr., Durham, NC 27709 (e-mail: bdodson@unither.com).

1040-0605/18 Copyright © 2018 the American Physiological Society

Downloaded from journals.physiology.org/journal/ajplung at Stanford Univ Med Ctr (171.066.010.174) on January 1, 2021.

Growth of the pulmonary vasculature is essential for distal lung growth during late development. Inhibiting angiogenesis in newborn rats decreases pulmonary artery density and impairs alveolarization (31). Previous work by our group has shown that alveolarization and pulmonary vascular density are both decreased in a sheep model of IUGR (61). Although angiogenesis is a complex process coordinated by several growth and transcriptional factors, hemodynamic stimuli, and signals from the extracellular matrix (ECM), we found that experimental IUGR has discrete, direct effects on pulmonary artery endothelial cell (PAEC) function. PAECs derived from IUGR fetal sheep demonstrate impaired proliferation, migration, and tube formation in association with downregulation of VEGF and nitric oxide signaling pathways (61). However, molecular mechanisms that alter PAEC function and disrupt pulmonary angiogenesis in IUGR remain incompletely understood.

Accumulating evidence suggests that the NF-κB signaling pathway may be a key driver of angiogenesis in the developing lung (30). The NF-κB family of transcription factors is ubiquitously expressed but remains sequestered in the cytoplasm in an inactive state in association with inhibitory IκB proteins (1). Activation of NF-κB by a complex of kinases, including IκB kinase α and β (IKKα and IKKβ), causes degradation of the IκB proteins and rapid nuclear translocation of active NF-κB complexes. Although best recognized for its role in regulating innate immunity and inflammation, the NF-κB pathway also has important roles during development (7, 28, 56, 74). Our prior studies showed that endogenous activation of the NF-κB pathway in the developing mouse lung promotes pulmonary angiogenesis and alveolarization and regulates VEGF receptor 2 (VEGFR2) expression in the pulmonary endothelium (30). However, whether disrupted NF-κB signaling in pulmonary endothelium contributes to decreased angiogenesis and alveolarization associated with IUGR is not known.

To identify signaling pathways that are dysregulated and may contribute to abnormal endothelial function in the IUGR lung, we performed unbiased, transcriptomic profiling of fetal PAECs derived from an experimental model IUGR induced by chronic placental insufficiency (59, 72). Using this approach, we identified marked decreases in NF-κB signaling in fetal IUGR PAECs and show that this reduction in NF-κB signaling is due to decreased gene expression of key NF-κB subunits and suppression of NF-κB inducible activation. We further found altered expression of ECM proteins that are regulated by NF-κB, suggesting that disruption of NF-κB-mediated ECM remodeling may contribute to abnormal lung and vascular development in IUGR.

METHODS

Experimental sheep model of IUGR. Pregnant Columbia-Rambouillet mixed-breed ewes (singleton pregnancies) were purchased from Nebeker Ranch (Lancaster, CA), housed, cared for, managed in compliance with the United States Department of Agriculture, the American Association for Accreditation for Laboratory Animal Care at the Perinatal Research Center at the University of Colorado (Aurora, CO), and approved by University of Colorado Institutional Animal Care and Use Committee (101924). The previously described sheep model of IUGR was created by exposing pregnant ewes to ambient hyperthermia (40°C for 12 h and 35°C for 12 h) from *day 35* to *day 110* during the 148-day gestation. Control animals were maintained in normothermic conditions at 25°C ambient temperature in otherwise identical living conditions. Food intake was matched to the IUGR group. On *day 135* (±2 days) of gestation, the ewe was sedated by ketamine (17.5 mg/kg iv) and diazepam (0.2 mg/kg iv) and euthanized by an injection of Fatal-Plus (Vortec Pharmaceuticals, Dearborn, MI) (85 mg/kg iv). In addition, the fetus was euthanized by an intra-cardiac injection of Fatal-Plus (250 mg/kg). Lungs were harvested for either histology or the isolation of PAECs, as previously published (61). The number of individual animals and technical replicates used for each experiment are detailed in the figure legends.

Lung fixation and immunofluorescent staining. Lung tissue was inflation fixed with 4% paraformaldehyde (wt/vol) in phosphate-buffered saline at 30 cmH_2O pressure. Lungs were ligated while under pressure and stored in 70% ethanol. Fixed lung tissue was paraffin embedded and sectioned. Tissue sections were deparafinized and rehydrated. Lung tissue immunofluorescent staining was performed as previously described using primary antibodies to detect NF-κB p65 (1:200; Santa Cruz Biotechnology, Santa Cruz) and the endothelial specific marker, CD31 (1:200 Dianova), and cell nuclei were stained with DAPI (30). Fluorescent images were captured using a Leica DM5500 upright microscope and a CoolSNAP fluorescent camera using HC Plan Apo 25-mm objective at ×10 magnification, and images were processed using Metamorph image analysis software. Sections obtained from three to four animals per experimental group were immunostained, and 5 fields of view/animal were imaged at ×20 and ×40 magnification.

PAEC isolation and culture. Primary PAECs were isolated from the left and right pulmonary proximal arteries as previously described (61). Endothelial cell phenotype was confirmed by positive immunostaining for the endothelial specific markers von Willebrand factor, vascular-endothelial cadherin, and endothelial nitric oxide synthase and negative staining for the smooth muscle cell markers, α-smooth muscle cell actin and desmin. PAECs from *passages 3–6* were used for all experiments. PAECs obtained from individual animals were kept separate throughout all passages and for all experiments described. Cells were cultured in DMEM with 10% fetal bovine serum (FBS) and 1% antibiotic, antimicrobial.

Gene array analysis and RNA validation. Total RNA was isolated from subconfluent PAECs, control ($n = 3$, 2 male, 1 female) and IUGR ($n = 4$, 2 male, 2 female), using TRIzol phenol extraction. RNA concentration and purity was determined by NanoDrop analysis (Thermo Fisher Scientific, Waltham MA) and 250 ng of RNA was used for sheep-specific gene microarrays (Affymetrix, Santa Clara, CA). Data were analyzed using R statistical software with the Bioconductor Gene Set Enrichment Analysis (GSEA) (normalized enrichment score to compare differences in gene sets and a false discovery rate <25%) plugin and ingenuity pathway analysis (analyzed upstream regulator analysis, mechanistic networks, causal network analysis, and downstream effects analysis, $P < 0.001$).

Based on GSEA analysis, specific genes were confirmed by quantitative PCR, using the primers listed in Table 1. cDNA was amplified using Transcriptor First Strand cDNA Synthesis Kit (Roche, Mannheim, Germany) in a standard thermocycler. cDNA samples were then assayed in triplicate using FastStart Essential DNA Green Master Kit (Roche) in a Lightcycler 96 (Roche) and the respective $2^{(-\Delta\Delta CT)}$ values were calculated using S15 as a housekeeping gene.

Electrophoretic mobility shift assays. Nuclear extracts were obtained from cultured PAECs ($n = 4$ for control PAECs, 1 male and 3 females; $n = 5$ for IUGR PAECs, 1 male and 4 females) using the NE-PER Kit (Pierce, Rockford, IL). The protein concentration was determined by the Bradford method. Ten micrograms of nuclear protein were used for binding reactions using γ-^{32}P-labeled oligonucleotides containing the κB consensus sequence (Promega, Madison, WI) in a binding buffer containing 500 ng of salmon sperm DNA, 0.01 U of poly(dI-dC), and 0.5 mM DTT (EMD Chemicals) as previously described (30). Supershift experiments were conducted with the addition of 2 μl of anti-p65, p50, p52, cRel, and RelB antibodies (Santa Cruz Biotechnology) to the nuclear extracts 30 min before the addition of the radiolabeled probe. Nuclear extracts were incubated with radiolabeled κB oligonucleotides at room temperature

Downloaded from journals.physiology.org/journal/ajplung at Stanford Univ Med Ctr (171.066.010.174) on January 1, 2021.

Table 1. *Primer sequences used for qPCR validation of genes identified in the microarray analysis*

Gene	RefSeq	Amplicon	Length, base pairs		Sequence 5′→3′
S15	XM_015096022.1	1–146	146	FWD	ATC ATT CTG CCC GAG ATG GTG
				REV	CGG GCC GGC CAT GTC TTA CG
BIRC2 (cIAP1)	XM_004015974.2	2314–2393	99	FWD	GGT GGC TTA AGG TGT TGG GA
				REV	CTC CTG CCC TTT CAT GCG TA
BIRC3 (cIAP2)	XM_012095321.1	96–250	176	FWD	CTC CTT AGG CCG GTC TCC T
				REV	TCC TCT CTT TTG TAA AAC GGC A
TNFAIP3 (A20)	XM_012131627.1	2455–2714	260	FWD	GGA CTG AAG AGC AGC TGA GGT
				REV	GCC ATT GCA CTT GGT GTT GC
CLFAR (cFLIP)	XM_004004820.2	2588–2807	239	FWD	GCT CCT GGA ACT CCA CAC TG
				REV	TCA AAG TCC CTC TGC TCC AC
NFKB1 (p50)	XM_004009667.2	3442–3551	109	FWD	CTT CCA TCC TGG AAC CAC TAA A
				REV	CAC CTC TCT GTC ATC ACT CTT G
RelA	XM_012102355.1	1107–1198	91	FWD	GTT CAG GGC TTC CTT CCT TAT T
				REV	GTA AAT CGG AAC TCT GGG AGC
MALT1	XM_012120865.1	1124–1347	243	FWD2	AGT GGA ATG CAC CGA AGA TGA
				REV2	ACG GCG TTA CGC ATC TCA TA
BTK	XM_012146742.1	1122–1347	245	FWD	GCA GTG GAA TGC ACC GAA GA
				REV	ACG GCG TTA CGC ATC TCA TA
LAMA4	XM_012182567	968–1104	136	FWD	TGG CAC AGA AGA TGC TTG AGG AGA
				REV	AGT GTC ATT GTA CTG CCT CTG CCA
COL4A1	XM_015098012.1	430–617	187	FWD	TGG CAT CAA AGG AGA AGC AGG TCT
				REV	CCA CAT CGC CCT TTG AAC CTT TCT
COL1A1	XM_015098715.1	889–981	92	FWD	AAT GGA GCT CCT GGT CAG AT
				REV	ATC ATT TCC TCG AGC ACC AG

BIRC3, baculoviral IAP repeat containing protein 3; CFLAR, CASP8 and FADD-like apoptosis regulator; COL1A1, collagen 1α1; *Col4α1*, collagen 4α1; *Lama4,* laminin α4; MALT1, mucosa associated lymphoid tissue lymphoma translocation gene 1; NFKB1, NF-κB1; TNFAIP3, TNF-α-induced protein 3; BTK, Bruton's tyrosine kinase.

for 30 min and electrophoresed on 6% polyacrylamide gels. To distinguish nonspecific binding of the nuclear proteins, competition reactions were performed by adding a 100-fold excess nonradiolabeled κB probe as done previously (2).

PAEC growth assay. Fetal PAECs were plated at 1×10^5 cells/well into six-well plates and allowed to adhere overnight in DMEM with 10% FBS. The following day (*day 0*), the cells were washed three times with PBS. DMEM with 2.5% FBS was added, and cells were incubated in room air (21% oxygen). Media was changed daily, and cell counts were performed on *day 0* and *day 5* after removing cells with trypsin digestion. All conditions were run in triplicate for each animal cell line (control: $n = 3$, 1 male and 2 females; IUGR: $n = 3$, 1 male and 2 females).

In vitro angiogenesis assay. The ability of fetal PAECs (control: $n = 3$, 1 male and 2 females; IUGR: $n = 3$, 1 male and 2 females) to form vascular structures in vitro was assayed by plating PAECs on a cross-linked collagen gel. PAECs were seeded at a density of 5×10^4 cells/well in 0.5% FBS DMEM, and each condition was tested in quadruplicate for each animal. PAECs are incubated for 24 h in room air (21% oxygen). Branch-point counting was performed in blinded fashion under ×10 magnification from each of four wells, with 3 to 4 fields of view obtained per well.

Modulation of NF-κB activity. NF-κB activity was modulated using two approaches. First, NF-κB activity was pharmacologically inhibited using BAY 11-7082 (BAY), a targeted IKKα and IKKβ inhibitor, as previously reported (30). Second, NF-κB activity was induced in fetal control and IUGR sheep PAECs (control: $n = 3$, 1 male and 2 females; IUGR: $n = 3$, 1 male and 2 females) by incubating the cells with LPS (10 ng/ml; *Escherichia coli* 055:B55, no. L2880 diluted into culture media; Sigma Chemical, St. Louis, MO) for 1 or 2 h (70). NF-κB and IKKβ activation were then assessed by Western blot analysis to detect nuclear p50 and p65 or determination of IKKβ activation by ELISA, as described in detail below.

Western immunoblot analysis. PAECs were lysed in ice-cold lysis buffer (50 mM Tris, pH 7.4, 1 mM EDTA, and 1 mM EGTA) with dissolved protease (Roche, Basel, Switzerland) and phosphatase inhibitors (PhosSTOP, Roche). Whole cell protein, cytoplasmic protein, and nuclear extract samples were quantified by Bradford DC protein assay (Bio-Rad, Hercules, CA). For analysis, a 30-μg sample was loaded into a Novex 4–12% gradient Bis-Tris gel (Thermo Fisher Scientific) and separated by electrophoresis. Proteins were transferred from the gel to PVDF membranes (Thermo Fisher Scientific). Blots were blocked in Li-Cor Odyssey blocking buffer (Li-Cor Biosciences, Lincoln, NE) for 1 h at room temperature and washed in Tris-buffered saline-Tween 20. Immunoblot detection of IKKα (1:1,000; Cell Signaling, Danvers, MA; no. 2682), IKKβ (1:1,000; Cell Signaling; no. 2678), p65 (1:1,000; Cell Signaling; no. 8242), p50 (1:1,000; Abcam, Cambridge, MA; no. ab7971), and β-actin (1:10,000; MP Biomedicals, Santa Ana, CA; no. 8691001) were detected using Li-Cor anti-mouse (no. 925-32212) and anti-rabbit (no. 925-68071) antibodies at concentrations of 1:7,500 in Odyssey buffer. The blots were imaged using the Odyssey CLx (Li-Cor Biosciences) and analyzed by Image Studio for Odyssey for CLx (Li-Cor Biosciences). Raw values were normalized to their respective β-actin loading control values and then reported as fold-change over control.

IKKβ activation assay. Identification of phosphorylated (active) levels of IKKβ protein were determined by ELISA assays to detect phosphorylation at Ser^{177} and Ser^{181} using the PathScan Phospho-IKKβ (Ser^{177}/Ser^{181}) Sandwich ELISA Kit no. 7080 (Cell Signaling Technology) per manufacturer's protocols. Spectrophotometric values (absorbance at 450 nm) were determined in control and IUGR PAECs at baseline and 1 and 2 h after treatment with LPS (10 ng/ml).

Statistical analysis. The number of enriched gene sets that were significant were indicated by a false discovery rate of <25%, following the recommendation by GSEA computation tool. Those gene sets with a nominal P value of <1% received further investigation (68). The ingenuity pathway analysis was completed using a suite of algorithms and tools for inferring and scoring regulator networks as previously described (38). For all other studies, results are expressed as means ± SE. Differences between two groups were determined using a *t*-test for normally distributed samples and Mann-Whitney for samples without normal distribution. For analysis with two independent variables, statistical significance was determined using two-way

Downloaded from journals.physiology.org/journal/ajplung at Stanford Univ Med Ctr (171.066.010.174) on January 1, 2021.

Table 2. *Altered pathways of interest identified by microarray analysis*

	Enrichment/Z-Score	*P* Value	Method
Collagen fibril organization	2.35	<0.01	Gene ontology analysis
Extracellular matrix	2.04	<0.01	Gene ontology analysis
IGF-1 signaling	0.82	<0.01	Ingenuity pathway analysis
VEGF signaling	−0.45	=0.02	Ingenuity pathway analysis
NF-κB	−1.63	<0.01	Gene set enrichment analysis
IKK2 signaling	−1.87	<0.01	Gene ontology analysis
Glucose metabolism disorder	−3.05	<0.01	Ingenuity pathway analysis

analysis of variance, followed by Sidak's multiple comparisons analysis. Statistical significance was defined as a P value of <0.05. All nonbioinformatics statistical analysis was done using GraphPad Prism version 6 (GraphPad Software, LaJolla, CA).

RESULTS

Microarray analysis identifies abnormalities in NF-κB signaling and ECM remodeling in IUGR PAECs. We previously found that the angiogenic function of PAECs obtained from IUGR fetal sheep was significantly decreased compared with PAECs from control sheep (61). However, the molecular mechanisms accounting for this angiogenic defect are not known. To address this question, we performed unbiased gene expression profiling in control and IUGR PAECs using sheep specific microarrays. Gene ontogeny and pathway analyses of the differentially expressed genes identified the enrichment of genes in association with specific metabolic, angiogenic, and ECM pathways (Table 2). Differences in gene expression included decreases in glucose metabolism and VEGF signaling, including *Vegfa* and *Vegfr2*, consistent with abnormalities in these same pathways we described previously (61). We also identified increases in ECM and collagen fibril organization pathways in the IUGR PAECs that are similar to changes that we observed in the systemic vasculature in our fetal sheep IUGR model (23). These include an increased expression of fibrosis-related genes, such as collagen1α1, and decreased basement membrane genes, including collagen 4α1 (*Col4α1*) and laminin α4 (*Lama4*). In addition, analyses of the microarray data identified significant suppression of NF-κB signaling, including decreased expression of individual NF-κB subunits (e.g., p50 and p65) and decreased gene expression of prosurvival NF-κB downstream targets (e.g., baculoviral IAP repeat containing protein 3 and CASP8 and FADD-like apoptosis regulator). Expression of the genes in the GSEA pathway showed NF-κB genes to be minimally expressed as shown in heat map form (Fig. 1*A*, red is the normalized high gene expression, and blue is the normalized low gene expression).

Using quantitative PCR, we confirmed specific dysregulation of the genes identified by the microarrays in these pathways of interest and found strong agreement between the two assays, thereby confirming significant downregulation of the NF-κB subunits p50 and p65 and the ECM components *Col4α1* and *Lama4* (Fig. 1*B*).

NF-κB expression and activity are decreased in IUGR fetal sheep and PAECs. We previously showed that endogenous NF-κB activity is high in the pulmonary endothelium of mice at the onset of alveolarization, and inhibiting NF-κB compromises angiogenic function of primary pulmonary endothelial cells obtained from the early alveolar murine lung (30). Therefore, we hypothesized that suppression of NF-κB signaling in IUGR fetal sheep may contribute to impaired angiogenesis in this model. Thus, we assessed the degree of active NF-κB in

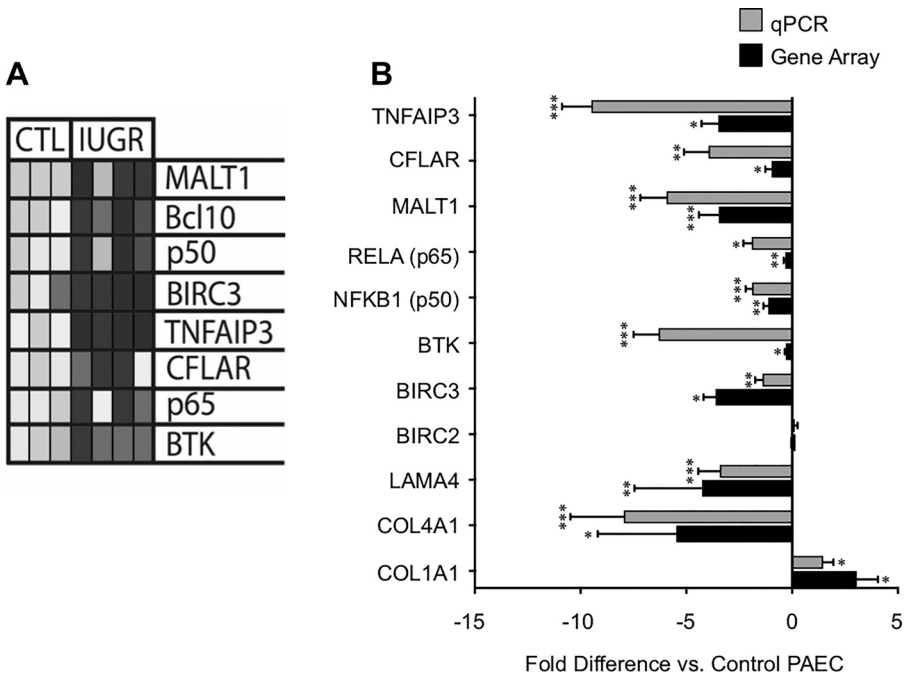

Fig. 1. Microarray analysis identifies abnormalities in NF-κB signaling and extracellular matrix pathways in intrauterine growth restriction (IUGR) pulmonary artery endothelial cells (PAECs). *A*: heat map of hierarchical cluster analysis showing dysregulated genes in the NF-κB pathway in control and IUGR PAECs. Light shading indicates increased expression, whereas dark shading indicates decreased expression. *B*: validation of dysregulated genes identified by microarray (dark bars) using quantitative PCR (qPCR) (light bars). Data presented are means ± SE, with control $n = 3$ and IUGR $n = 4$ for the microarray and $n = 4$ animals with 3 replicates of each for the qPCR. $^{*}P < 0.05$, $^{**}P < 0.01$, and $^{***}P < 0.001$. BIRC3, baculoviral IAP repeat containing protein 3; CFLAR, CASP8 and FADD-like apoptosis regulator; COL1A1, collagen 1α1; COL4A1, collagen 4α1; CTL, control; LAMA4, laminin α4; MALT1, mucosa associated lymphoid tissue lymphoma translocation gene 1; TNFAIP3, TNF-α-induced protein 3; RELA, v-rel avian reticuloendotheliosis viral oncogene homolog A; BTK, Bruton's tyrosine kinase.

Downloaded from journals.physiology.org/journal/ajplung at Stanford Univ Med Ctr (171.066.010.174) on January 1, 2021.

control and IUGR fetal sheep lungs in situ by immunostaining to detect active nuclear NF-κB complexes. Similar to past findings in the developing murine lung, there was striking evidence of active nuclear NF-κB complexes throughout the lungs of control fetal sheep (Fig. 2), including strong expression within CD31 positive endothelial cells in the distal pulmonary vasculature (Fig. 2, high magnification *inset*). In contrast, staining for NF-κB complexes was greatly diminished in the lungs of IUGR fetal sheep, including a paucity of nuclear staining within the endothelial cells of the distal vasculature (Fig. 2).

We confirmed this difference in endothelial NF-κB activation by performing electrophoretic mobility shift assays on nuclear extracts obtained from PAECs isolated from control and IUGR fetal sheep to detect NF-κB-DNA binding. NF-κB-DNA binding was present in all the control PAECs, consisting of both an upper and lower complex (Fig. 2*B*). In contrast, NF-κB-DNA binding was completely absent in three primary cell lines of IUGR PAECs and diminished in the remaining two cell lines. Quantification of these differences by densitometry identified a 68% reduction in NF-κB-DNA binding in the IUGR PAECs as compared with control PAECs ($P < 0.05$) (Fig. 2*C*). We also performed supershift analysis to identify the composition of the two complexes present by preincubating the nuclear extracts with antibodies specific for the NF-κB family members p50 and p65 before incubation with the radiolabeled NF-κB oligonucleotide. Using this method, we found that the upper complex was shifted upward with the addition of antibodies against either the p65 or the p50 subunit, identifying this complex as the heterodimer of p65p50.

Inducible activation of IKKs is impaired in IUGR compared with control PAECs despite similar levels of IKKα and IKKβ. To explore mechanisms underlying the difference in NF-κB activation between control and IUGR PAECs, we first compared the expression of the two main NF-κB activating kinases, IKKα and IKKβ. Using Western blot analysis, we found that the baseline levels of IKKα and IKKβ were no different in IUGR compared with control PAECs (Fig. 3*A* and *B*). We then assessed IKKβ activation with an ELISA that detects phosphorylation of IKKβ at serine residues Ser^{177} and Ser^{181}, which are key steps in IKKβ activation (14). IKKβ activity was similar in unstimulated control and IUGR PAECs at baseline (Fig. 3*C*). In response to LPS stimulation, both control and IUGR PAECs activated IKKβ at 1 h. Although IKKβ activity remained elevated in control PAECs at 2h, it was significantly lower in IUGR PAECs at this time point.

Baseline expression and LPS-mediated nuclear translocation of NF-κB subunits p65 and p50 are decreased in IUGR PAECs. We next determined nuclear and cytoplasmic levels of p65 and p50 in control and PAECs at baseline and in response

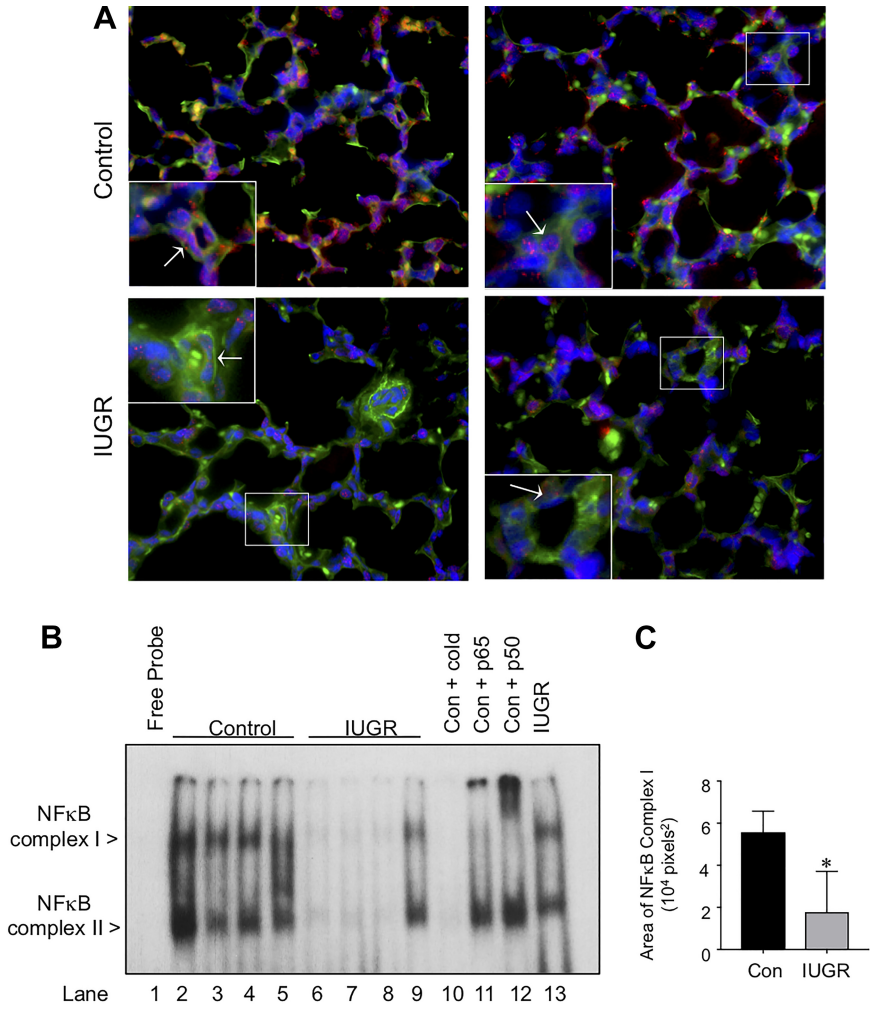

Fig. 2. Active NF-κB is higher in the lungs and pulmonary artery endothelial cells (PAECs) of control fetal sheep as compared with intrauterine growth restriction (IUGR) fetal sheep. *A*: representative immunofluorescent images from control and IUGR fetal lung from two separate animals per group, stained to detect the NF-κB subunit, p65 (red), the endothelial specific marker, CD31 (green), and chromatin (blue). The *insets* show higher magnification images of distal vessels in the four animals. *B*: EMSA was performed using nuclear extracts obtained from control (*lanes 2–5*) and IUGR PAECs (*lanes 6–9*), incubated with radiolabeled κB oligonucleotides. Specificity of the bands in control PAECs (*lane 2* sample) was confirmed by the disappearance of the bands with the addition of 100-fold excess of cold oligonucleotide (*lane 10*). Supershift analysis of the NF-κB complexes present in control PAECs (*lane 2* sample) was then performed by preincubating the nuclear extracts with antibodies against p65 (*lane 11*) and p50 (*lane 12*). For Complex I, a shift upward was produced by the addition of p65 antibodies and p50 antibodies. *C*: quantification of EMSA by Image J to measure the total area the Complex I band in each sample. Data presented are means ± SE, with $n = 4$ for control PAECs and $n = 5$ for IUGR PAECs $*P = 0.02$ vs. control. Con, control.

Downloaded from journals.physiology.org/journal/ajplung at Stanford Univ Med Ctr (171.066.010.174) on January 1, 2021.

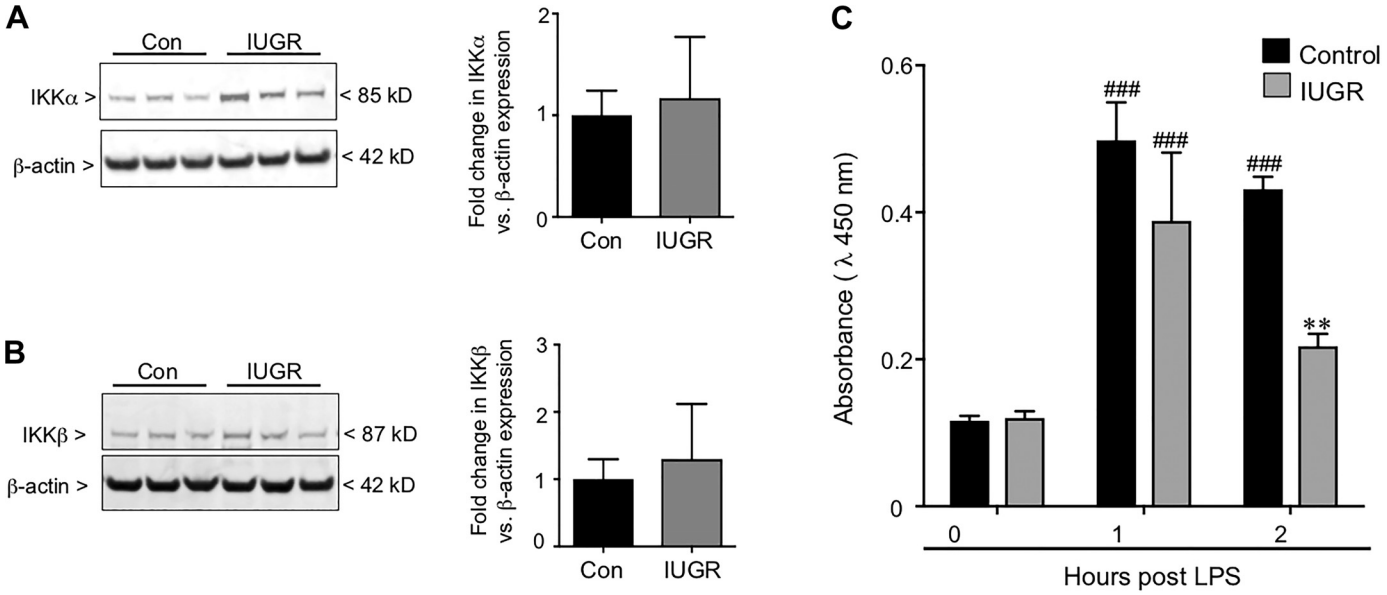

Fig. 3. Inducible activation of IKKβ is impaired in intrauterine growth restriction (IUGR) compared with control pulmonary artery endothelial cells (PAECs) despite similar levels of IKKα and IKKβ. IKKα (*A*) and IKKβ (*B*) protein levels were detected by western immunoblot, with $n = 3$ animals with 3 technical replicates per group. Relative expression of IKKα and IKKβ were normalized to β-actin and expressed as fold-change over control. Data presented are means ± SE, with $n = 3$ animals for each group. Phosphorylation of IKKβ (*C*) was determined by ELISA in control and IUGR PAECs at baseline and at 1 or 2 h after LPS (10 ng/ml) stimulation. Data presented are means ± SE, with $n = 3$ animals with 2 technical replicates for each group. ###$P < 0.001$ vs. 0 h, and **$P = 0.002$ vs. control. Con, control.

to stimulation with LPS, an activator of NF-κB signaling. In control PAECs, cytoplasmic levels of p65 (Fig. 4*A*) and p50 (Fig. 4*B*) are decreased 1 h after stimulation with LPS, and nuclear levels of both subunits are increased at 1 and 2 h (Fig. 4*C* and *D*), which is consistent with translocation of active p65p50 heterodimers into the nucleus. In contrast, IUGR PAECs had significantly lower amounts of cytoplasmic p65 and p50 than control PAECs at baseline and marked reductions in nuclear levels of p65 and p50 1 and 2 h after LPS stimulation, consistent with reduced inducible activation of NF-κB in IUGR PAECs.

Angiogenic functions are suppressed in IUGR PAECs to levels measured in control PAECs after treatment with BAY 11-7082, an inhibitor of NF-κB signaling. We next compared the capacity of the control and IUGR PAECs to proliferate and form tube structures in vitro at baseline and after treatment with a selective and pharmacological inhibitor of the IKK activating kinases, BAY 11-7082 (2, 29, 30). At baseline, proliferation of IUGR PAECs in response to DMEM was significantly lower than that observed in the control PAECs (Fig. 5*A*). Treatment of the control PAECs with BAY resulted in dose-dependent decreases in PAEC proliferation. In contrast, BAY treatment had no effect on the proliferation of the IUGR PAECs. We also performed in vitro tube formation assays and found that tube formation was impaired in vehicle-treated IUGR PAECs as compared with control PAECs (Fig. 5*B*). BAY treatment also markedly decreased tube formation in control PAECs, suppressing branch points to values obtained with IUGR PAECs at baseline. In contrast, BAY treatment had no further reduction on tube formation in the IUGR PAECs.

DISCUSSION

To determine potential molecular mechanisms associated with abnormal lung endothelial function in IUGR, we used unbiased gene expression profiling to compare differences in PAECs from normal fetal sheep and an established model of IUGR. Using this strategy, we found that IUGR significantly suppresses endogenous NF-κB activation in fetal pulmonary endothelium, and we attributed this decrease in pathway activation to both decreases in the expression of key NF-κB subunits (p65 and p50) and to defects in IKKβ-mediated, inducible NF-κB activation. IUGR also decreased the expression of *Col4α1* and *Lama4*, putative downstream targets of NF-κB that are essential basement membrane components. The importance of endogenous NF-κB activation in the fetal sheep PAECs was further highlighted by demonstrating that inhibiting IKKβ in control PAECs disrupts angiogenic function to a degree similar to the impaired angiogenesis observed in the IUGR PAECs in baseline conditions. In concert with our prior studies, this report provides additional evidence in a robust animal model of disrupted alveolarization and angiogenesis that endogenous NF-κB activity in pulmonary endothelial cells is essential for late lung development.

Pulmonary angiogenesis is essential for the growth and development of the distal lung. In premature infants dying from BPD, angiogenic factors are decreased, and the pulmonary vasculature is dysmorphic (8, 19, 26). Inhibition of angiogenesis impairs lung growth, decreases pulmonary artery density, and causes pulmonary hypertension (31), whereas augmenting lung angiogenesis with inhaled nitric oxide (45) or exogenous VEGF (39, 40, 71) preserves alveolarization in experimental models of BPD. Mechanisms through which VEGF enhances alveolar growth include the release of angiocrine factors that act on the developing alveolar epithelium, such as retinoic acid (76) and hepatocyte growth factor (64).

In addition, our prior studies identified high levels of endogenous activation of NF-κB in the pulmonary endothelium of the early alveolar mouse lung in vivo and showed that inhibi-

Downloaded from journals.physiology.org/journal/ajplung at Stanford Univ Med Ctr (171.066.010.174) on January 1, 2021.

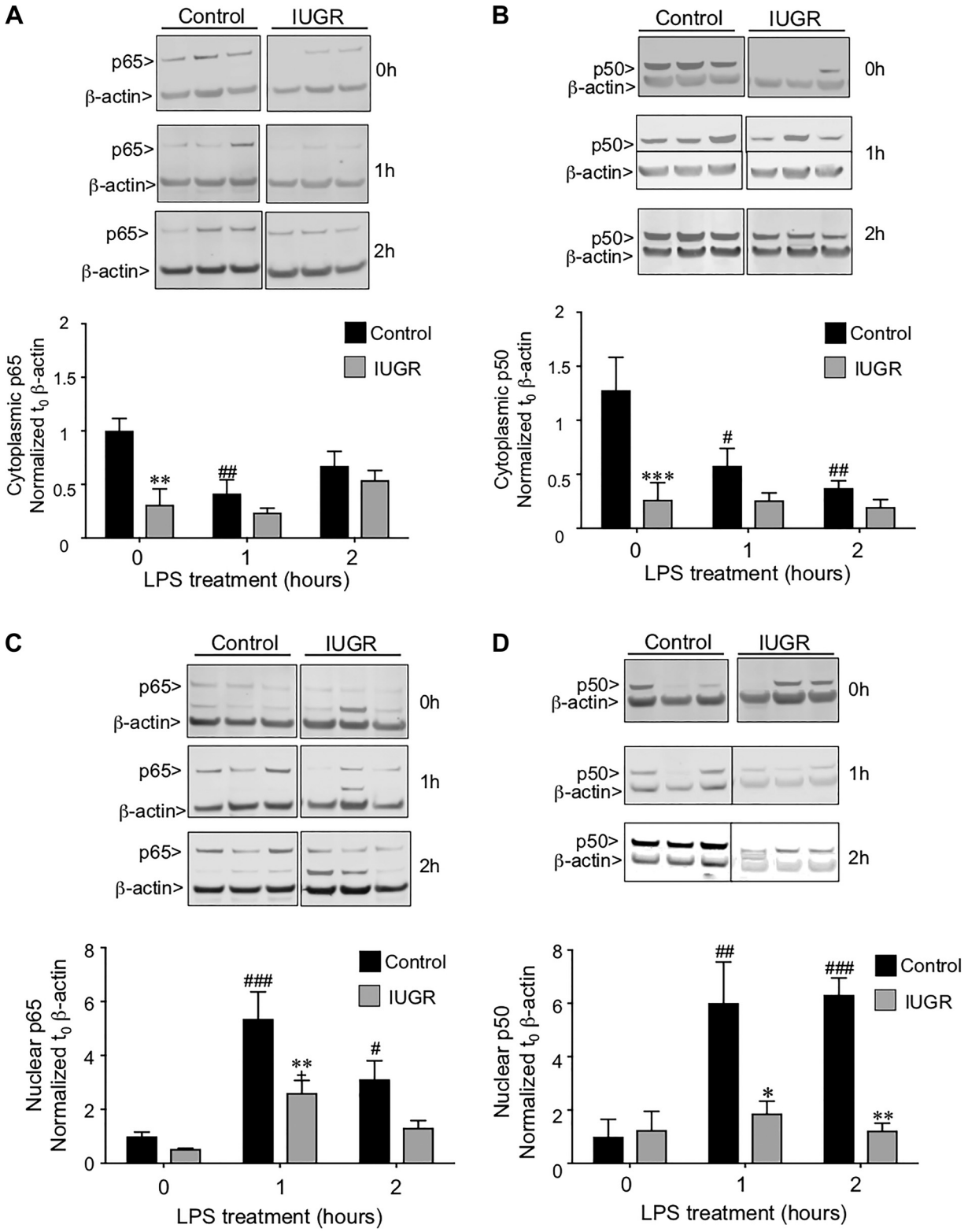

Fig. 4. Baseline cytoplasmic expression and LPS-mediated nuclear translocation of NF-κB subunits p65 and p50 are decreased in intrauterine growth restriction (IUGR) pulmonary artery endothelial cells (PAECs). Representative images and densitometric quantification of western immunoblot analysis was used to detect the levels of cytoplasmic p65 (*A*), cytoplasmic p50 (*B*), nuclear p65 (*C*), and nuclear p50 (*D*). Data presented are means ± SE, with $n = 3$–4 per group with values for each target protein normalized to β-actin at *time 0* (t_0). $^{**}P = 0.002$ and $\#\#P = 0.006$ vs. control PAECs at *0 h* (*A*); $^{***}P < 0.001$, $\#P = 0.02$, and $\#\#P = 0.002$ vs. control PAECs at *0 h* (*B*); $^{**}P = 0.007$ vs. control PAECs at *1 h*, $\#\#\#P < 0.001$ and $\#\#P = 0.004$ vs. control PAECs at *0 h*, and $+P = 0.04$ vs. IUGR PAECs at *0 h* (*C*); and $^{*}P = 0.01$ vs. control PAECs at *1 h*, $^{**}P = 0.001$ vs. control PAECs at *2 h*, $\#\#P = 0.001$ and $\#\#\#P < 0.001$ vs. control PAECs at *0 h* (*D*).

Downloaded from journals.physiology.org/journal/ajplung at Stanford Univ Med Ctr (171.066.010.174) on January 1, 2021.

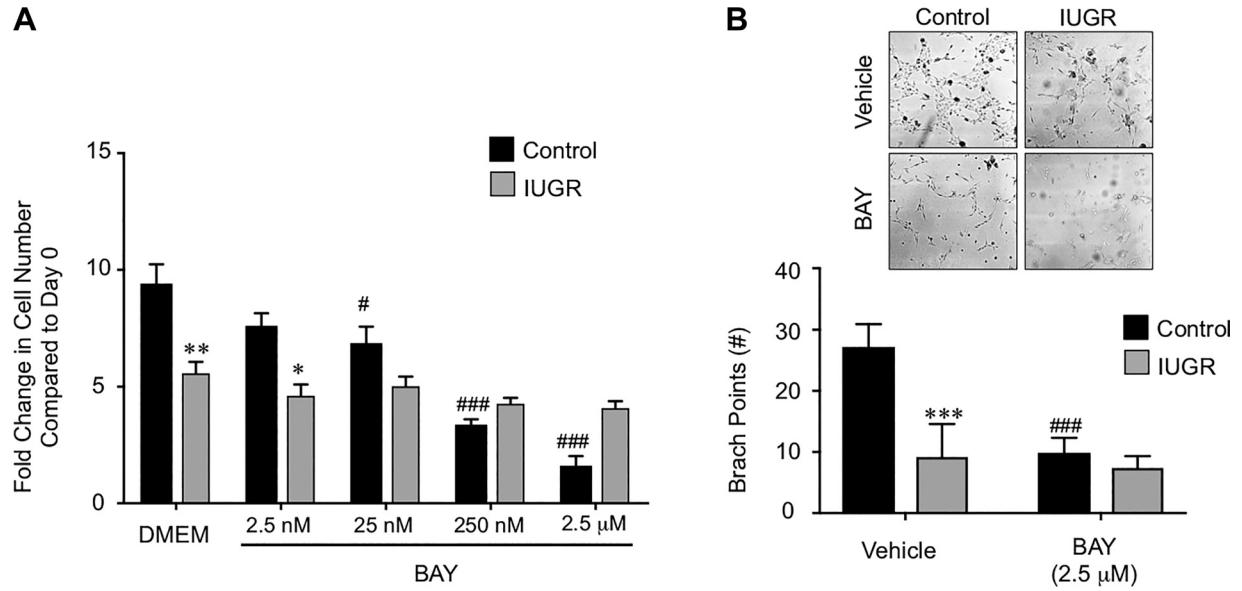

Fig. 5. Inhibition of NF-κB reduces control of pulmonary artery endothelial cell (PAEC) angiogenic function to levels similar to the impaired angiogenesis observed in intrauterine growth restriction (IUGR) PAECs. *A*: proliferation assays were performed on control (dark bars) and IUGR (light bars) PAECs in response to DMEM + vehicle. In similar studies, proliferation was measured in control and IUGR PAECs treated with increasing doses of the IKK inhibitor, BAY 11-7082 (BAY). Data shown are means ± SE, with $n = 3$ cell lines from different animals with 3–4 replicates performed per cell isolation. $^{*}P < 0.05$ and $^{**}P < 0.01$ vs. control PAECs treated with the same stimulus, and $\#P < 0.05$ and $\#\#\#P < 0.001$ vs. control DMEM-treated. *B*: in vitro tube formation assays were performed by plating control and IUGR PAECs on cross-linked collagen. At 18 h, images were obtained, and the number of branch points per ×10 field magnification were determined in a blinded fashion. Data presented are means ± SE, with $n = 18$–30 fields counted from PAECs isolated from 3 separate animals per experimental group. $^{***}P < 0.001$ and $\#\#\#P < 0.001$ vs. vehicle treated control PAECs.

tion of NF-κB in primary murine pulmonary endothelial cells decreases VEGFR2 expression and reduces PAEC function in vitro (30). These original findings are supported by observations that lung growth in transgenic mice with sustained NF-κB signaling is preserved in response to hyperoxia-induced injury (52). In addition, female newborn mice exposed to hyperoxia have better lung structure when compared with male mice, which is associated with enhanced NF-κB signaling (46). This latter observation may partly explain clinical observations of sex-related differences for BPD risk and severity in premature infants (9, 16). Moreover, a recent study that performed proteomic analysis of murine lungs from embryonic to adult stages of development identified NF-κB-regulated networks as a key signaling pathway increased during the transition from the prenatal to the postnatal period (55). In the present report, we further report suppression of the IKK/NF-κB signaling pathway in a fetal sheep model of IUGR that is characterized by decreased fetal lung vascular and alveolar growth, which is independent of hyperoxia exposure. These findings provide additional support for the hypothesis that early disruption of NF-κB signaling impairs pulmonary angiogenesis and alveolarization across multiple species and in response to both prenatal and postnatal injury and for the paradigm that NF-κB is a central regulator of pulmonary vascular development.

We found that combined gene set enrichment, gene ontology, and ingenuity pathway analyses implicated NF-κB as a top decreased pathway in IUGR PAECs when compared with controls. Although IKKα and IKKβ gene expression was not different in control versus IUGR PAECs, genes both upstream and downstream of the IKKs were significantly decreased in IUGR cells. These data suggest that while IKK gene expression is preserved in IUGR PAECs, IKK activity may be decreased. In addition, the expression of p65 and p50, components of the transcriptionally active p65p50 heterodimer, was significantly decreased in IUGR PAECs. Consistent with these results, prosurvival (e.g., baculoviral IAP repeat containing protein 3 and CASP8 and FADD-like apoptosis regulator) and proinflammatory [e.g., TNF-α-induced protein 3 (TNFAIP3)] genes, which are downstream of NF-κB, are decreased in IUGR PAECs.

In addition, immunofluorescent staining of nuclear (active) p65 in situ was decreased in IUGR lungs in comparison with controls. Assessment of NF-κB-DNA binding by EMSA further confirmed a significant reduction in the binding of p65p50 heterodimers, which are NF-κB complexes that we previously identified as playing a key role to upregulate VEGFR2 expression in the developing mouse endothelium (30). Overall, these data are consistent with our hypothesis that reduced activation of the NF-κB pathway is an important mechanism underlying the angiogenic defect induced by IUGR.

In addition to alterations in the NF-κB signaling pathway, microarray analysis also identified alterations in genes involved in the ECM and collagen fibril organization pathways, including decreased *Col4α1* and *Lama4* expression, which are both key components of the basement membrane (BM) and regulators of angiogenesis. The ECM is continuously remodeled during lung development (69), serving as a scaffold that influences numerous cellular processes, and dysregulated ECM remodeling has been demonstrated in experimental models of aberrant lung development (54). BM components can provide either pro- or antiangiogenic cues. Although mature networks of BM maintain blood vessel quiescence by inhibiting endothelial proliferation and migration, during remodeling, the exposure of different domains modulates endothelial cell phe-

Downloaded from journals.physiology.org/journal/ajplung at Stanford Univ Med Ctr (171.066.010.174) on January 1, 2021.

notype to promote angiogenesis (35). In human microvascular endothelial cells, type IV collagen secretion increases during angiogenesis (4). In addition, type IV collagen promotes neovessel length and stability in a dose-dependent fashion in aortic explants (10). Simultaneous disruption of *Lama4* and *Lama1* in zebrafish impairs development of the intersegmental vessels (57), and *Lama4* deletion in mice impairs corneal angiogenesis and microvascular maturation (73). Moreover, disruption of these key BM components may directly affect lung development. Although mice with homozygous deletions of both *Col4a1* and *Col4a2* die during midembryogenesis because of widespread impairments of basement membrane stability (58), mice with heterozygous mutations in *Col4a1* frequently die in the perinatal period, exhibiting respiratory distress and cyanosis and compact lungs that contain few terminal airspaces (27). *Col4a1* mutant mice that survive the perinatal period have lungs with simplified alveoli at P6, and emphysematous changes at P30, in association with alterations in myofibroblast proliferation and differentiation (50). Taken together, these data suggest that the decreases of *Col4α1* and *Lama4* expression in our model could be directly contributing to the impaired angiogenesis and alveolarization observed in this experimental model of IUGR.

Moreover, the alterations in NF-κB and ECM signaling observed in IUGR may be interrelated. For example, the ECM can influence NF-κB activation by changing the clustering and engagement of specific cell surface integrins. Specifically, the αvβ3 integrin appears to play an important role in mediating endothelial angiogenic functions, in part through NF-κB-mediated effects. Integrin αvβ3 is highly expressed by angiogenic but not quiescent blood vessels (12), and blocking αvβ3 integrin signaling with antibodies disrupts both embryonic and tumor angiogenesis, in part by inducing endothelial cell apoptosis (13). In rat aortic endothelial cells, αvβ3 promotes endothelial cell survival by activating NF-κB (63). Although intact type IV collagen binds α1β1 integrins, proteolytic cleavage during ECM remodeling reveals a cryptic site that allows binding of αvβ3 integrins (75). Similarly, *Lama4* mediates endothelial cell adhesion through the αvβ3 integrin, and this interaction promotes angiogenesis in chick chorioallantoic membrane assays (43) and in Matrigel plug assays performed in nude mice (25). Both *Col4α1* and *Lama4* contain κB binding sequences in their promoters, indicating that they are putative NF-κB transcriptional targets. Taken together, these data raise the possibility that in this IUGR model, decreased expression of *Col4α1* and *Lama4* could contribute to the suppression of NF-κB activation, or, alternatively, that the downregulation of NF-κB transcriptional activity decreases the expression of these specific ECM components.

The limitations of this study must be acknowledged. Cryopreserved cell lines from previous studies were used for the array analysis, without matching sexes in the samples. Research has shown sex-related differences in NF-κB signaling in the developing mouse lung (46). Although in this study the samples were not specifically matched based on sex, similar ratios of male and female animals were distributed between the two experimental groups (gene array analysis, control PAECs: 2 males and 1 female and IUGR PAECs: 2 males and 2 females; EMSA, control PAECs: 1 male and 3 females and IUGR PAECs: 1 male and 4 females; and in vitro and western analyses, control PAECs: 1 male and 2 females and IUGR PAECs: 1 male and 2 females). Future studies designed specifically to determine the influence of sex on suppressed NF-κB signaling in IUGR would be necessary to know whether there are similar sex-specific differences in the lungs of fetal sheep. NF-κB is a complex signaling pathway considered a "master regulator" because of its ability to regulate diverse cellular responses by promoting or repressing the transcription of hundreds of target genes in a cell- and stimulus-specific fashion. Furthermore, the NF-κB activating kinases, IKKα and IKKβ, have been shown to exert NF-κB independent effects, altering the activation states of other transcription factors and influencing transcription by altering chromatin remodeling (1). In this study, it is not possible to differentiate between NF-κB-mediated effects resulting from the decreased expression of p65 and p50 and IKKβ-mediated, NF-κB-independent effects resulting from the decreased activation of IKKβ. Future studies employing ChIP-Seq strategies to identify specific p50 and p65 regulated genes in the fetal sheep PAECs may be helpful in further delineating the specific effects of the two limbs of this pathway. Although we show that inhibition of NF-κB signaling in control PAECs inhibits angiogenesis, definitive experiments to rescue the impaired NF-κB signaling in the IUGR PAECs were not performed. Given that these cells exhibit both a defect in IKKβ activation and repressed expression of the p65 and p50 subunits, an effective rescue strategy would necessarily entail the overexpression of a constitutively active IKKβ construct and p65 and p50 constructs. The downstream effects of NF-κB activation are cell- and stimulus-specific and are influenced by timing of activation and development. Thus, a more granular understanding of the mechanisms allowing for physiological effects for NF-κB in the developing pulmonary endothelium lung is essential, given that pathological activation of NF-κB can have detrimental effects (1, 70). Although, many therapeutic strategies aimed at limiting pathological NF-κB activation have been developed (3, 6), the development of strategies to enhance NF-κB has not received similar focus. Potential strategies that could be effective in enhancing NF-κB-mediated angiogenesis in the pulmonary vasculature include the modulation of micro RNAs that modulate NF-κB subunit expression (22, 77); increasing the activity of factors which alter the acetylation of p65, allowing for nuclear retention of NF-κB complexes (41); and high throughput screens of the Food and Drug Administration approved drug, compound, and/or siRNA libraries to identify novel activators of NF-κB in reporter cell lines.

In summary, the present study identifies suppression of IKK/NF-κB signaling as a key mechanism contributing to the impaired pulmonary endothelial angiogenic function observed in IUGR. In addition to decreasing the expression of key NF-κB subunits, IUGR also impaired inducible activation of the NF-κB pathway and decreased the expression of numerous putative NF-κB downstream targets, including BM components important angiogenesis. These data add to our prior work identifying endogenous activation of NF-κB as an important regulator of pulmonary angiogenesis during late lung development and are the first, to our knowledge, to identify endothelial-specific suppression of NF-κB signaling in an established, experimental model of impaired angiogenesis and alveolarization induced by IUGR. Despite advances in the treatment of infants with IUGR, pulmonary outcomes remain a major clinical problem with little change in incidence in recent decades

Downloaded from journals.physiology.org/journal/ajplung at Stanford Univ Med Ctr (171.066.010.174) on January 1, 2021.

(24, 32). Given that alveolarization continues for years after birth, we speculate that the suppression of NF-κB activity in response to IUGR could contribute to the higher incidence of BPD and long-term deficits in pulmonary function observed in premature patients with IUGR. Thus, the development of targeted strategies to selectively restore NF-κB activity in the developing pulmonary endothelium may represent a potential strategy to enhance pulmonary angiogenesis and alveolarization in patients with IUGR.

ACKNOWLEDGMENTS

We thank the Genomics and Microarray Core at the University of Colorado Anschutz Medical Campus for their assistance in preparing and running mRNA arrays. Dr. Dodson is currently at United Therapeutics. The work contained was completed at the University of Colorado Denver, Anschutz Medical Campus and Stanford University.

GRANTS

This work was supported by grants from the Children's Hospital Colorado Research Scholar Award (to R. B. Dodson); the Entelligence Young Investigator Award (to R. B. Dodson); Stanford Child Health Research Institute Tashia and John Morgridge Faculty Scholar Award (to C. M. Alvira); NIH National Heart, Lung, and Blood Institute (NHLBI) Grant R01-HL-122918 (to C. M. Alvira); NIH National Institute of Diabetes and Digestive and Kidney Diseases Grant R01-DK-088139 (to P. J. Rozance); and NIH NHLBI Grant R01-HL-68702 (to S. H. Abman).

DISCLOSURES

No conflicts of interest, financial or otherwise, are declared by the authors.

AUTHOR CONTRIBUTIONS

R.B.D., J.G., T.M.C., S.H.A., and C.M.A. conceived and designed research; R.B.D., K.N.P., G.S., and C.M.A. performed experiments; R.B.D., K.N.P., J.G., P.J.R., G.S., D.A., K.J., T.M.C., S.H.A., and C.M.A. analyzed data; R.B.D., K.N.P., P.J.R., T.M.C., S.H.A., and C.M.A. interpreted results of experiments; R.B.D., S.H.A., and C.M.A. prepared figures; R.B.D. and C.M.A. drafted manuscript; R.B.D., K.N.P., J.G., P.J.R., D.A., T.M.C., S.H.A., and C.M.A. edited and revised manuscript; R.B.D., K.N.P., J.G., P.J.R., G.S., D.A., K.J., T.M.C., S.H.A., and C.M.A. approved final version of manuscript.

REFERENCES

1. **Alvira CM.** Nuclear factor-kappa-B signaling in lung development and disease: one pathway, numerous functions. *Birth Defects Res A Clin Mol Teratol* 100: 202–216, 2014. doi:10.1002/bdra.23233.
2. **Alvira CM, Abate A, Yang G, Dennery PA, Rabinovitch M.** Nuclear factor-kappaB activation in neonatal mouse lung protects against lipopolysaccharide-induced inflammation. *Am J Respir Crit Care Med* 175: 805–815, 2007. doi:10.1164/rccm.200608-1162OC.
3. **Awasthee N, Rai V, Chava S, Nallasamy P, Kunnumakkara AB, Bishayee A, Chauhan SC, Challagundla KB, Gupta SC.** Targeting IκappaB kinases for cancer therapy. *Semin Cancer Biol* S1044-579X(17)30046-9, 2018. doi:10.1016/j.semcancer.2018.02.007.
4. **Bahramsoltani M, Slosarek I, De Spiegelaere W, Plendl J.** Angiogenesis and collagen type IV expression in different endothelial cell culture systems. *Anat Histol Embryol* 43: 103–115, 2014. doi:10.1111/ahe.12052.
5. **Barker DJ, Godfrey KM, Fall C, Osmond C, Winter PD, Shaheen SO.** Relation of birth weight and childhood respiratory infection to adult lung function and death from chronic obstructive airways disease. *BMJ* 303: 671–675, 1991. doi:10.1136/bmj.303.6804.671.
6. **Begalli F, Bennett J, Capece D, Verzella D, D'Andrea D, Tornatore L, Franzoso G.** Unlocking the NF-κB conundrum: embracing complexity to achieve specificity. *Biomedicines* 5: 50, 2017. doi:10.3390/biomedicines5030050.
7. **Belvin MP, Anderson KV.** A conserved signaling pathway: the Drosophila toll-dorsal pathway. *Annu Rev Cell Dev Biol* 12: 393–416, 1996. doi:10.1146/annurev.cellbio.12.1.393.
8. **Bhatt AJ, Pryhuber GS, Huyck H, Watkins RH, Metlay LA, Maniscalco WM.** Disrupted pulmonary vasculature and decreased vascular endothelial growth factor, Flt-1, and TIE-2 in human infants dying with bronchopulmonary dysplasia. *Am J Respir Crit Care Med* 164: 1971–1980, 2001. doi:10.1164/ajrccm.164.10.2101140.
9. **Binet ME, Bujold E, Lefebvre F, Tremblay Y, Piedboeuf B; Canadian Neonatal Network™.** Role of gender in morbidity and mortality of extremely premature neonates. *Am J Perinatol* 29: 159–166, 2012. doi:10.1055/s-0031-1284225.
10. **Bonanno E, Iurlaro M, Madri JA, Nicosia RF.** Type IV collagen modulates angiogenesis and neovessel survival in the rat aorta model. *In Vitro Cell Dev Biol Anim* 36: 336–340, 2000. doi:10.1290/1071-2690(2000)036<0336:TICMAA>2.0.CO;2.
11. **Bose C, Van Marter LJ, Laughon M, O'Shea TM, Allred EN, Karna P, Ehrenkranz RA, Boggess K, Leviton A; Extremely Low Gestational Age Newborn Study Investigators.** Fetal growth restriction and chronic lung disease among infants born before the 28th week of gestation. *Pediatrics* 124: e450–e458, 2009. doi:10.1542/peds.2008-3249.
12. **Brooks PC, Clark RA, Cheresh DA.** Requirement of vascular integrin alpha v beta 3 for angiogenesis. *Science* 264: 569–571, 1994. doi:10.1126/science.7512751.
13. **Brooks PC, Montgomery AM, Rosenfeld M, Reisfeld RA, Hu T, Klier G, Cheresh DA.** Integrin alpha v beta 3 antagonists promote tumor regression by inducing apoptosis of angiogenic blood vessels. *Cell* 79: 1157–1164, 1994. doi:10.1016/0092-8674(94)90007-8.
14. **Carter RS, Geyer BC, Xie M, Acevedo-Suárez CA, Ballard DW.** Persistent activation of NF-kappa B by the tax transforming protein involves chronic phosphorylation of IkappaB kinase subunits IKKbeta and IKKgamma. *J Biol Chem* 276: 24445–24448, 2001. doi:10.1074/jbc.C000777200.
15. **Chen CM, Wang LF, Su B.** Effects of maternal undernutrition during late gestation on the lung surfactant system and morphometry in rats. *Pediatr Res* 56: 329–335, 2004. doi:10.1203/01.PDR.0000134254.83113.8E.
16. **Costeloe K, Hennessy E, Gibson AT, Marlow N, Wilkinson AR; for the EPICure Study Group.** The EPICure study: outcomes to discharge from hospital for infants born at the threshold of viability. *Pediatrics* 106: 659–671, 2000. doi:10.1542/peds.106.4.659.
17. **Curle DC, Adamson IY.** Retarded development of noenatal rat lung by maternal malnutrition. *J Histochem Cytochem* 26: 401–408, 1978. doi:10.1177/26.5.659840.
18. **Dailey WA, Gryc W, Garg PG, Drenser KA.** Frizzled-4 variations associated with retinopathy and intrauterine growth retardation: a potential marker for prematurity and retinopathy. *Ophthalmology* 122: 1917–1923, 2015. doi:10.1016/j.ophtha.2015.05.036.
19. **De Paepe ME, Mao Q, Powell J, Rubin SE, DeKoninck P, Appel N, Dixon M, Gundogan F.** Growth of pulmonary microvasculature in ventilated preterm infants. *Am J Respir Crit Care Med* 173: 204–211, 2006. doi:10.1164/rccm.200506-927OC.
20. **Devaskar SU, Chu A.** Intrauterine growth restriction: hungry for an answer. *Physiology (Bethesda)* 31: 131–146, 2016. doi:10.1152/physiol.00033.2015.
21. **Dezateux C, Lum S, Hoo AF, Hawdon J, Costeloe K, Stocks J.** Low birth weight for gestation and airway function in infancy: exploring the fetal origins hypothesis. *Thorax* 59: 60–66, 2004.
22. **Dharap A, Pokrzywa C, Murali S, Pandi G, Vemuganti R.** MicroRNA miR-324-3p induces promoter-mediated expression of RelA gene. *PLoS One* 8: e79467, 2013. doi:10.1371/journal.pone.0079467.
23. **Dodson RB, Rozance PJ, Fleenor BS, Petrash CC, Shoemaker LG, Hunter KS, Ferguson VL.** Increased arterial stiffness and extracellular matrix reorganization in intrauterine growth-restricted fetal sheep. *Pediatr Res* 73: 147–154, 2013. doi:10.1038/pr.2012.156.
24. **Fanaroff AA, Stoll BJ, Wright LL, Carlo WA, Ehrenkranz RA, Stark AR, Bauer CR, Donovan EF, Korones SB, Laptook AR, Lemons JA, Oh W, Papile LA, Shankaran S, Stevenson DK, Tyson JE, Poole WK; NICHD Neonatal Research Network.** Trends in neonatal morbidity and mortality for very low birthweight infants. *Am J Obstet Gynecol* 196: 147.e1–147.e8, 2007. doi:10.1016/j.ajog.2006.09.014.
25. **Gonzalez AM, Gonzales M, Herron GS, Nagavarapu U, Hopkinson SB, Tsuruta D, Jones JC.** Complex interactions between the laminin alpha 4 subunit and integrins regulate endothelial cell behavior in vitro and angiogenesis in vivo. *Proc Natl Acad Sci USA* 99: 16075–16080, 2002. doi:10.1073/pnas.252649399.
26. **Gorenflo M, Vogel M, Obladen M.** Pulmonary vascular changes in bronchopulmonary dysplasia: a clinicopathologic correlation in short- and long-term survivors. *Pediatr Pathol* 11: 851–866, 1991. doi:10.3109/15513819109065482.

Downloaded from journals.physiology.org/journal/ajplung at Stanford Univ Med Ctr (171.066.010.174) on January 1, 2021.

27. **Gould DB, Phalan FC, van Mil SE, Sundberg JP, Vahedi K, Massin P, Bousser MG, Heutink P, Miner JH, Tournier-Lasserve E, John SW.** Role of COL4A1 in small-vessel disease and hemorrhagic stroke. *N Engl J Med* 354: 1489–1496, 2006. doi:10.1056/NEJMoa053727.
28. **Hayden MS, Ghosh S.** Signaling to NF-kappaB. *Genes Dev* 18: 2195–2224, 2004. doi:10.1101/gad.1228704.
29. **Hou Y, Liu M, Husted C, Chen C, Thiagarajan K, Johns JL, Rao SP, Alvira CM.** Activation of the nuclear factor-κB pathway during postnatal lung inflammation preserves alveolarization by suppressing macrophage inflammatory protein-2. *Am J Physiol Lung Cell Mol Physiol* 309: L593–L604, 2015. doi:10.1152/ajplung.00029.2015.
30. **Iosef C, Alastalo TP, Hou Y, Chen C, Adams ES, Lyu SC, Cornfield DN, Alvira CM.** Inhibiting NF-κB in the developing lung disrupts angiogenesis and alveolarization. *Am J Physiol Lung Cell Mol Physiol* 302: L1023–L1036, 2012. doi:10.1152/ajplung.00230.2011.
31. **Jakkula M, Le Cras TD, Gebb S, Hirth KP, Tuder RM, Voelkel NF, Abman SH.** Inhibition of angiogenesis decreases alveolarization in the developing rat lung. *Am J Physiol Lung Cell Mol Physiol* 279: L600–L607, 2000. doi:10.1152/ajplung.2000.279.3.L600.
32. **Jobe AJ.** The new BPD: an arrest of lung development. *Pediatr Res* 46: 641–643, 1999. doi:10.1203/00006450-199912000-00007.
33. **Joss-Moore LA, Wang Y, Yu X, Campbell MS, Callaway CW, McKnight RA, Wint A, Dahl MJ, Dull RO, Albertine KH, Lane RH.** IUGR decreases elastin mRNA expression in the developing rat lung and alters elastin content and lung compliance in the mature rat lung. *Physiol Genomics* 43: 499–505, 2011. doi:10.1152/physiolgenomics.00183.2010.
34. **Joyce BJ, Louey S, Davey MG, Cock ML, Hooper SB, Harding R.** Compromised respiratory function in postnatal lambs after placental insufficiency and intrauterine growth restriction. *Pediatr Res* 50: 641–649, 2001. doi:10.1203/00006450-200111000-00018.
35. **Kalluri R.** Basement membranes: structure, assembly and role in tumour angiogenesis. *Nat Rev Cancer* 3: 422–433, 2003. doi:10.1038/nrc1094.
36. **Karadag A, Sakurai R, Wang Y, Guo P, Desai M, Ross MG, Torday JS, Rehan VK.** Effect of maternal food restriction on fetal rat lung lipid differentiation program. *Pediatr Pulmonol* 44: 635–644, 2009. doi:10.1002/ppul.21030.
37. **Kavurt S, Özcan B, Aydemir O, Bas AY, Demirel N.** Risk of retinopathy of prematurity in small for gestational age premature infants. *Indian Pediatr* 51: 804–806, 2014. doi:10.1007/s13312-014-0506-9.
38. **Krämer A, Green J, Pollard J Jr, Tugendreich S.** Causal analysis approaches in Ingenuity Pathway Analysis. *Bioinformatics* 30: 523–530, 2014. doi:10.1093/bioinformatics/btt703.
39. **Kunig AM, Balasubramaniam V, Markham NE, Morgan D, Montgomery G, Grover TR, Abman SH.** Recombinant human VEGF treatment enhances alveolarization after hyperoxic lung injury in neonatal rats. *Am J Physiol Lung Cell Mol Physiol* 289: L529–L535, 2005. doi:10.1152/ajplung.00336.2004.
40. **Kunig AM, Balasubramaniam V, Markham NE, Seedorf G, Gien J, Abman SH.** Recombinant human VEGF treatment transiently increases lung edema but enhances lung structure after neonatal hyperoxia. *Am J Physiol Lung Cell Mol Physiol* 291: L1068–L1078, 2006. doi:10.1152/ajplung.00093.2006.
41. **Lee H, Herrmann A, Deng JH, Kujawski M, Niu G, Li Z, Forman S, Jove R, Pardoll DM, Yu H.** Persistently activated Stat3 maintains constitutive NF-kappaB activity in tumors. *Cancer Cell* 15: 283–293, 2009. doi:10.1016/j.ccr.2009.02.015.
42. **Lee JW, VanderVeen D, Allred EN, Leviton A, Dammann O.** Prethreshold retinopathy in premature infants with intrauterine growth restriction. *Acta Paediatr* 104: 27–31, 2015. doi:10.1111/apa.12799.
43. **Lian J, Dai X, Li X, He F.** Identification of an active site on the laminin alpha4 chain globular domain that binds to alphavbeta3 integrin and promotes angiogenesis. *Biochem Biophys Res Commun* 347: 248–253, 2006. doi:10.1016/j.bbrc.2006.06.069.
44. **Lin Y, Lechner AJ.** Surfactant content and type II cell development in fetal guinea pig lungs during prenatal starvation. *Pediatr Res* 29: 288–291, 1991. doi:10.1203/00006450-199103000-00013.
45. **Lin YJ, Markham NE, Balasubramaniam V, Tang JR, Maxey A, Kinsella JP, Abman SH.** Inhaled nitric oxide enhances distal lung growth after exposure to hyperoxia in neonatal rats. *Pediatr Res* 58: 22–29, 2005. doi:10.1203/01.PDR.0000163378.94837.3E.
46. **Lingappan K, Jiang W, Wang L, Moorthy B.** Sex-specific differences in neonatal hyperoxic lung injury. *Am J Physiol Lung Cell Mol Physiol* 311: L481–L493, 2016. doi:10.1152/ajplung.00047.2016.
47. **Liu X, Lin Y, Tian B, Miao J, Xi C, Liu C.** Maternal protein restriction alters VEGF signaling and decreases pulmonary alveolar in fetal rats. *Int J Clin Exp Pathol* 7: 3101–3111, 2014.
48. **Longo S, Bollani L, Decembrino L, Di Comite A, Angelini M, Stronati M.** Short-term and long-term sequelae in intrauterine growth retardation (IUGR). *J Matern Fetal Neonatal Med* 26: 222–225, 2013. doi:10.3109/14767058.2012.715006.
49. **Lopuhaä CE, Roseboom TJ, Osmond C, Barker DJ, Ravelli AC, Bleker OP, van der Zee JS, van der Meulen JH.** Atopy, lung function, and obstructive airways disease after prenatal exposure to famine. *Thorax* 55: 555–561, 2000. doi:10.1136/thorax.55.7.555.
50. **Loscertales M, Nicolaou F, Jeanne M, Longoni M, Gould DB, Sun Y, Maalouf FI, Nagy N, Donahoe PK.** Type IV collagen drives alveolar epithelial-endothelial association and the morphogenetic movements of septation. *BMC Biol* 14: 59, 2016. [Erratum in: *BMC Biol* 14: 73, 2016. doi:10.1186/s12915-016-0297-7.] doi:10.1186/s12915-016-0281-2.
51. **Maritz GS, Cock ML, Louey S, Suzuki K, Harding R.** Fetal growth restriction has long-term effects on postnatal lung structure in sheep. *Pediatr Res* 55: 287–295, 2004. doi:10.1203/01.PDR.0000106314.99930.65.
52. **McKenna S, Michaelis KA, Agboke F, Liu T, Han K, Yang G, Dennery PA, Wright CJ.** Sustained hyperoxia-induced NF-κB activation improves survival and preserves lung development in neonatal mice. *Am J Physiol Lung Cell Mol Physiol* 306: L1078–L1089, 2014. doi:10.1152/ajplung.00001.2014.
53. **Metsälä J, Kilkkinen A, Kaila M, Tapanainen H, Klaukka T, Gissler M, Virtanen SM.** Perinatal factors and the risk of asthma in childhood—a population-based register study in Finland. *Am J Epidemiol* 168: 170–178, 2008. doi:10.1093/aje/kwn105.
54. **Mižíková I, Morty RE.** The extracellular matrix in bronchopulmonary dysplasia: target and source. *Front Med (Lausanne)* 2: 91, 2015. doi:10.3389/fmed.2015.00091.
55. **Moghieb A, Clair G, Mitchell HD, Kitzmiller J, Zink EM, Kim YM, Petyuk V, Shukla A, Moore RJ, Metz TO, Carson J, McDermott JE, Corley RA, Whitsett JA, Ansong C.** Time-resolved proteome profiling of normal lung development. *Am J Physiol Lung Cell Mol Physiol* 315: L11–L24, 2018. doi:10.1152/ajplung.00316.2017.
56. **Perkins ND.** Integrating cell-signalling pathways with NF-kappaB and IKK function. *Nat Rev Mol Cell Biol* 8: 49–62, 2007. doi:10.1038/nrm2083.
57. **Pollard SM, Parsons MJ, Kamei M, Kettleborough RN, Thomas KA, Pham VN, Bae MK, Scott A, Weinstein BM, Stemple DL.** Essential and overlapping roles for laminin alpha chains in notochord and blood vessel formation. *Dev Biol* 289: 64–76, 2006. doi:10.1016/j.ydbio.2005.10.006.
58. **Pöschl E, Schlötzer-Schrehardt U, Brachvogel B, Saito K, Ninomiya Y, Mayer U.** Collagen IV is essential for basement membrane stability but dispensable for initiation of its assembly during early development. *Development* 131: 1619–1628, 2004. doi:10.1242/dev.01037.
59. **Regnault TR, Orbus RJ, Battaglia FC, Wilkening RB, Anthony RV.** Altered arterial concentrations of placental hormones during maximal placental growth in a model of placental insufficiency. *J Endocrinol* 162: 433–442, 1999. doi:10.1677/joe.0.1620433.
60. **Reiss I, Landmann E, Heckmann M, Misselwitz B, Gortner L.** Increased risk of bronchopulmonary dysplasia and increased mortality in very preterm infants being small for gestational age. *Arch Gynecol Obstet* 269: 40–44, 2003. doi:10.1007/s00404-003-0486-9.
61. **Rozance PJ, Seedorf GJ, Brown A, Roe G, O'Meara MC, Gien J, Tang JR, Abman SH.** Intrauterine growth restriction decreases pulmonary alveolar and vessel growth and causes pulmonary artery endothelial cell dysfunction in vitro in fetal sheep. *Am J Physiol Lung Cell Mol Physiol* 301: L860–L871, 2011. doi:10.1152/ajplung.00197.2011.
62. **Sasi A, Abraham V, Davies-Tuck M, Polglase GR, Jenkin G, Miller SL, Malhotra A.** Impact of intrauterine growth restriction on preterm lung disease. *Acta Paediatr* 104: e552–e556, 2015. doi:10.1111/apa.13220.
63. **Scatena M, Almeida M, Chaisson ML, Fausto N, Nicosia RF, Giachelli CM.** NF-kappaB mediates alphavbeta3 integrin-induced endothelial cell survival. *J Cell Biol* 141: 1083–1093, 1998. doi:10.1083/jcb.141.4.1083.
64. **Seedorf G, Metoxen AJ, Rock R, Markham N, Ryan S, Vu T, Abman SH.** Hepatocyte growth factor as a downstream mediator of vascular endothelial growth factor-dependent preservation of growth in the developing lung. *Am J Physiol Lung Cell Mol Physiol* 310: L1098–L1110, 2016. doi:10.1152/ajplung.00423.2015.
65. **Seikku L, Rahkonen L, Tikkanen M, Hämäläinen E, Rahkonen P, Andersson S, Teramo K, Paavonen J, Stefanovic V.** Amniotic fluid

Downloaded from journals.physiology.org/journal/ajplung at Stanford Univ Med Ctr (171.066.010.174) on January 1, 2021.

erythropoietin and neonatal outcome in pregnancies complicated by intrauterine growth restriction before 34 gestational weeks. *Acta Obstet Gynecol Scand* 94: 288–294, 2015. doi:10.1111/aogs.12553.

66. **Sharma D, Farahbakhsh N, Shastri S, Sharma P.** Intrauterine growth restriction - part 2. *J Matern Fetal Neonatal Med* 29: 4037–4048, 2016. doi:10.3109/14767058.2016.1154525.
67. **Soudée S, Vuillemin L, Alberti C, Mohamed D, Becquet O, Farnoux C, Biran V, Baud O.** Fetal growth restriction is worse than extreme prematurity for the developing lung. *Neonatology* 106: 304–310, 2014. doi:10.1159/000360842.
68. **Subramanian A, Tamayo P, Mootha VK, Mukherjee S, Ebert BL, Gillette MA, Paulovich A, Pomeroy SL, Golub TR, Lander ES, Mesirov JP.** Gene set enrichment analysis: a knowledge-based approach for interpreting genome-wide expression profiles. *Proc Natl Acad Sci USA* 102: 15545–15550, 2005. doi:10.1073/pnas.0506580102.
69. **Surate Solaligue DE, Rodríguez-Castillo JA, Ahlbrecht K, Morty RE.** Recent advances in our understanding of the mechanisms of late lung development and bronchopulmonary dysplasia. *Am J Physiol Lung Cell Mol Physiol* 313: L1101–L1153, 2017. doi:10.1152/ajplung.00343.2017.
70. **Tang JR, Michaelis KA, Nozik-Grayck E, Seedorf GJ, Hartman-Filson M, Abman SH, Wright CJ.** The NF-κB inhibitory proteins IκBα and IκBβ mediate disparate responses to inflammation in fetal pulmonary endothelial cells. *J Immunol* 190: 2913–2923, 2013. doi:10.4049/jimmunol.1202670.
71. **Thébaud B, Ladha F, Michelakis ED, Sawicka M, Thurston G, Eaton F, Hashimoto K, Harry G, Haromy A, Korbutt G, Archer SL.** Vascular endothelial growth factor gene therapy increases survival, promotes lung angiogenesis, and prevents alveolar damage in hyperoxia-induced lung injury: evidence that angiogenesis participates in alveolarization. *Circulation* 112: 2477–2486, 2005. doi:10.1161/CIRCULATIONAHA.105.541524.
72. **Thureen PJ, Trembler KA, Meschia G, Makowski EL, Wilkening RB.** Placental glucose transport in heat-induced fetal growth retardation. *Am J Physiol* 263: R578–R585, 1992.
73. **Thyboll J, Kortesmaa J, Cao R, Soininen R, Wang L, Iivanainen A, Sorokin L, Risling M, Cao Y, Tryggvason K.** Deletion of the laminin alpha4 chain leads to impaired microvessel maturation. *Mol Cell Biol* 22: 1194–1202, 2002. doi:10.1128/MCB.22.4.1194-1202.2002.
74. **Vallabhapurapu S, Karin M.** Regulation and function of NF-kappaB transcription factors in the immune system. *Annu Rev Immunol* 27: 693–733, 2009. doi:10.1146/annurev.immunol.021908.132641.
75. **Xu J, Rodriguez D, Petitclerc E, Kim JJ, Hangai M, Moon YS, Davis GE, Brooks PC.** Proteolytic exposure of a cryptic site within collagen type IV is required for angiogenesis and tumor growth in vivo. *J Cell Biol* 154: 1069–1079, 2001. [Erratum in *J Cell Biol* 155: 859, 2001.] doi:10.1083/jcb.200103111.
76. **Yun EJ, Lorizio W, Seedorf G, Abman SH, Vu TH.** VEGF and endothelium-derived retinoic acid regulate lung vascular and alveolar development. *Am J Physiol Lung Cell Mol Physiol* 310: L287–L298, 2016. doi:10.1152/ajplung.00229.2015.
77. **Zhao XD, Lu YY, Guo H, Xie HH, He LJ, Shen GF, Zhou JF, Li T, Hu SJ, Zhou L, Han YN, Liang SL, Wang X, Wu KC, Shi YQ, Nie YZ, Fan DM.** MicroRNA-7/NF-κB signaling regulatory feedback circuit regulates gastric carcinogenesis. *J Cell Biol* 210: 613–627, 2015. doi:10.1083/jcb.201501073.

Downloaded from journals.physiology.org/journal/ajplung at Stanford Univ Med Ctr (171.066.010.174) on January 1, 2021.